Paper

Optimization of 40 Gbit/s soliton-based TDM systems by Q-map method

Member Kazuhiro Shimoura (Kansai Electric Power Co.)
Member Ikuo Yamashita (Kansai Electric Power Co.)
Member Shigeyuki Seikai (Kansai Electric Power Co.)

Q-map method is a practical method for the design of high-speed optical communication systems. We applied this method to the optimization of periodically dispersion compensated 40 Gbit/s soliton-based TDM systems. The optimum dispersion compensation is about ±30 ps/nm and does not depend on the compensation periods. In a single-channel 640-km transmission experiment using conventional dispersion shifted fibers and 2-pieces of dispersion compensation fibers, we observed error free transmission in the wavelength range of 1.2-nm by adjusting the location of the dispersion compensation elements. The optimal channel power is about +7 dBm and the transmissible condition shows good agreement with the numerical simulations. We applied these techniques to 80 Gbit/s (40 Gbit/s, 2 PDM) transmission line design and observed error free 800 km transmission. In 40 or 80 Gbit/s/fiber systems, the dispersion-managed soliton scheme is attractive because higher SN-ratio, conventional dispersion shifted fibers and narrow band low cost amplifiers are applicable. The soliton stabilization effect enables stable long distance transmission.

Keywords: optical communication, dispersion compensation, simulation, soliton, Q-map

1. Introduction

Simulation modeling of TDM and WDM systems has become an important issue in the design of high-speed optical communication lines [(1)(2)]. Q-maps are the contour mappings of Q-factor on the system parameter spaces, and we can easily evaluate the optimal parameter values and their margins from Q-maps [(3)]. We should optimize many parameters simultaneously especially in the nonlinear transmission systems, and the Q-map method is a practical technique for the design of such systems. In 40 Gbit/s single-channel soliton based systems, over 10000 km transmission has achieved [(4)]. In this paper, we apply Q-map method to the optimization of 40 Gbit/s soliton-based TDM systems.

2. Q-map method

Q-factor represents the signal-to-noise ratio at the receiver decision circuit in voltage or current unit [(5)]. Fig.1 shows the Q-factor definition for RZ pulses. This definition considers soliton stability, interactions between pulses, timing jitter effects and other effects. In soliton-based systems using relatively higher signal power, we can use relatively short bit patterns because the stability of soliton pulses and nonlinear interactions between adjacent pulses are dominant compared to the pulse pattern effects and signal to noise ratio. We use 15 bit PRBS signals in the following simulations. The simulation code solves the nonlinear Schrödinger equation (NLS) using the split step Fourier method. The fiber attenuation rate is 0.2 dB/km, fiber effective core area is 50 μm^2, third order dispersion is +0.07 ps/nm^2/km and Kerr coefficient is 2.24×10^{-20} m^2/W for all cases. The bit error rate (BER) can be estimated from equation (1), and requires Q > 6 for the BER of 10^{-9}. This BER gives the upper limit for the signal because some degradation occurs in the demultiplexing circuit.

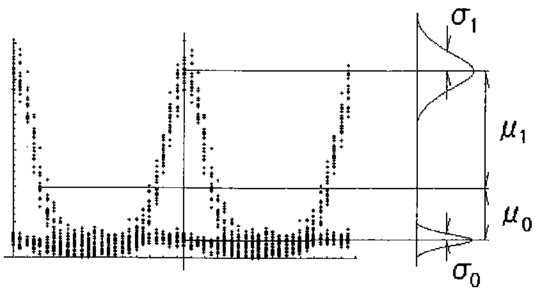

$$Q = \frac{\mu_0 + \mu_1}{\sigma_0 + \sigma_1}$$

σ : standard deviation
μ : mean value

Fig.1. Q-factor definition for RZ-pulses.

$$BER = \frac{1}{2} erfc\left(\frac{Q}{\sqrt{2}}\right) \approx \frac{\exp(-Q^2/2)}{Q\sqrt{2\pi}} \qquad (1)$$

3. High-speed TDM system design

3.1 Q-maps for 40 Gbit/s systems

We proposed some kinds of Q-maps for the design of periodically dispersion compensated lines, and found two extremely stable transmission conditions exist in this scheme [(6)]. In high-speed TDM systems, such as 40 Gbit/s systems, pulse width becomes narrow and signal power becomes large. The transmission characteristics of such systems are sensitive to the fiber average dispersion and dispersion compensation elements. Fig.2 shows the dispersion maps of periodically dispersion compensated lines. The dispersion-shifted fibers of dispersion D (ps/nm/km) and length La (km) are connected with optical amplifiers. A linear dispersion compensation element Dc (ps/nm) is installed in every Nc amplifier span, therefore the compensation length $Lc = La\ Nc$. The total transmission distance is Lt. The fiber dispersion D can be positive (anomalous dispersion type) or negative (normal dispersion type) values, and the average dispersion Dav (ps/nm/km) is calculated by the equation (2).

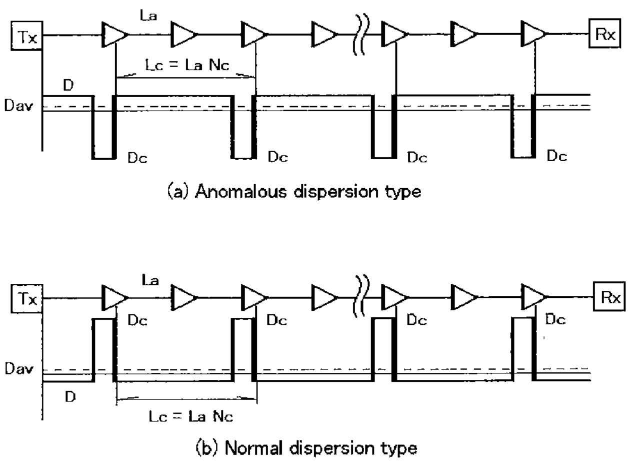

Fig. 2. Dispersion maps for the simulation analysis.

$$Dav = D + \frac{Dc}{Nc \cdot La} \tag{2}$$

A chirped Gaussian pulse of 7.5 ps FWHM is considered as the initial pulse. The time slot of 40 Gbit/s signal is 25 ps, therefore the duty ratio is 30 %.

$$\phi(0,\tau) = \sqrt{\frac{Pm}{A}}\ \exp\left[-\frac{\tau^2}{2T_0^2}(1 - iC)\right] \tag{3}$$

where Pm is the initial peak power of the pulse. The fiber input power Pav is related to Pm by $Pav = Pm - 8.0$ dBm, where pulse duty ratio of 30 % and mark ratio of 50 % are assumed. T_0 is the half-width at $1/e$-intensity point related with T_{FWHM} by $T_{FWHM} = 1.665\ T_0$. C is a frequency chirp parameter and represents up-chirp by $C < 0$ and down-chirp by $C > 0$.

The optimal dispersion management strength is estimated by the S-parameter calculated by the equation (4) for periodically dispersion compensated lines.

$$S = 2.55\ \frac{|Dc|}{T_S^{\,2}} \tag{4}$$

where Dc (ps/nm) is the dispersion compensation and Ts (ps) is the minimum pulse width (FWHM) at the chirp-free point. $S = 1.65$ gives the optimum strength of dispersion management for soliton systems because nonlinear interactions between adjacent pulses becomes minimal at this condition [7].

Fig.3 shows the Q-map on $Dav - Dc$ plane. The amplifier spacing $La = 50$ km, transmission distance $Lt = 3000$ km, and fiber input power $Pav = +5$ dBm ($Pm = +13$ dBm). A 6-nm width filter is installed in every amplifier and amplifier noise is not considered in these simulations. Two transmissible zones almost symmetrically appear in the anomalous dispersion area ($Dav > 0$). These areas are corresponding to the two types of lines of Fig.2. The optimal Dav is about +0.03 ps/nm/km. We can estimate the optimal strength of the dispersion management from this map and get $Dc = \pm 30$ ps/nm.

Fig.4 shows the Q-map on $Dav - Pav$ plane. We can estimate the optimal average dispersion Dav and fiber input power Pav from this figure. The optimal Dav is about +0.03 ps/nm/km and Pav is about +5 dBm. We can also estimate the system parameter margins from these Q-maps.

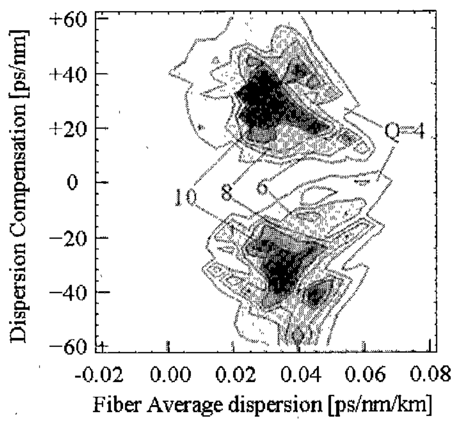

Fig. 3. Q-map on the Dav - Dc plane by 21 x 31 points. ($Nc = 2$, $La = 50$ km, $Lt = 3$ Mm, $Pav = +5$ dBm)

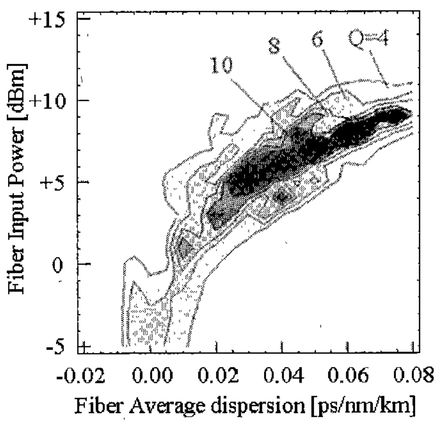

Fig. 4. Q-map on the Dav - Pav plane by 21 x 21 points. ($Nc = 2$, $La = 50$ km, $Lt = 3$ Mm, $Dc = +30$ ps/nm)

3.2 Design of the dispersion compensation elements

Figs. 5 show the Q-maps on *Dav* – *Dc* plane for *Nc* = 4 and *Nc* = 6 cases. Other parameters are identical to Fig. 3. The optimal *Dav* is about +0.03 ps/nm/km and the optimal *Dc* is about ±30 ps/nm. These values are almost the same as the *Nc* = 2 case in spite of the local dispersion *D* are different. In longer *Lc* case, *D* becomes smaller and signal distortion caused by FWM effect easily occurs along the *D* = 0 line.

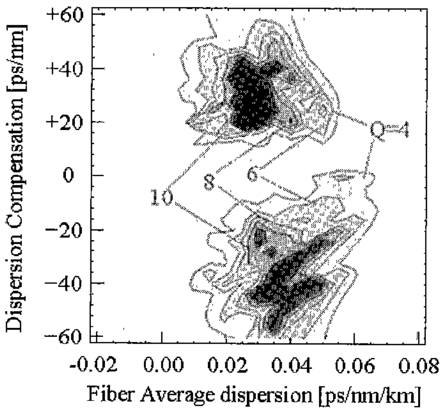

(a) *Nc* = 4

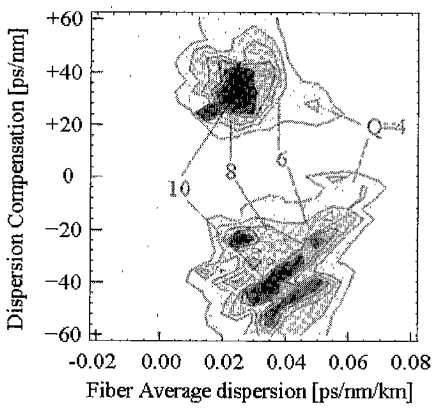

(b) *Nc* = 6

Fig. 5. Q-maps on the *Dav* - *Dc* plane for 40 Gbit/s lines. (*La* = 50 km, *Lt* = 3 Mm, *Pav* = +5 dBm)

Fig. 6 to Fig. 9 shows the Q-maps for different *La* cases. Fig. 6 and Fig. 7 are *La* = 30 km case, Fig. 8 and Fig. 9 are *La* = 80 km case. The optimal *Dc* is not strictly depending on the compensation period *Lc* because *S*-parameter only depends on *Ts* in the optimally designed lines. If the duty ratio is constant, the optimal *Dc* is determined only by the bit rate, and about ±30 ps/nm for 40 Gbit/s lines. This result simplifies the design of the dispersion compensation elements. The optimal average dispersion *Dav* and fiber input power *Pav* slightly depends on *La*. For longer *La* cases, optimal *Dav* becomes smaller and *Pav* becomes larger.

In soliton-based long-distance systems, *La* should be less than about 50 km because the soliton order *N* should be in the range of $0.5 < N < 1.5$ which means the maximum and minimum power ratio of the transmission should be less than 9 [8].

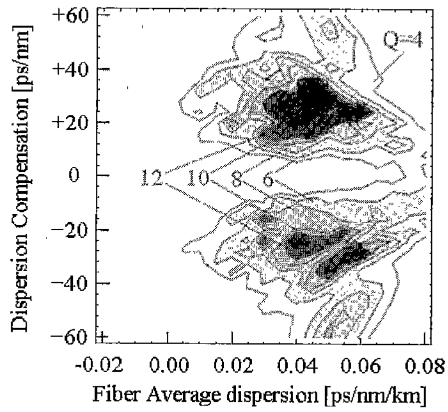

Fig. 6. Q-map on the *Dav* - *Dc* plane for 40 Gbit/s lines. (*Nc* = 2, *La* = 30 km, *Lt* = 3 Mm, *Pav* = +5 dBm)

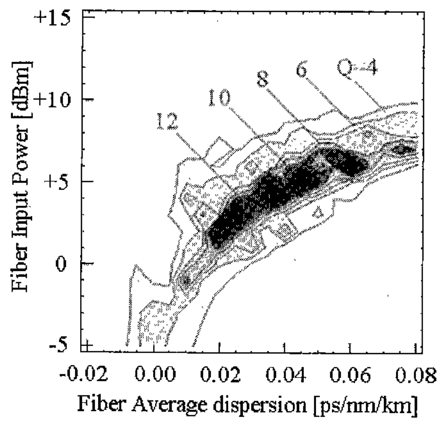

Fig. 7. Q-map on the *Dav* - *Pav* plane for 40 Gbit/s lines. (*Nc* = 2, *La* = 30 km, *Lt* = 3 Mm, *Dc* = +30 ps/nm)

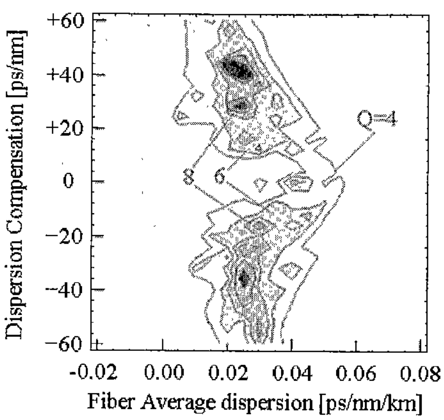

Fig. 8. Q-map on the *Dav*-*Dc* plane for 40 Gbit/s lines. (*Nc* = 2, *La* = 80 km, *Lt* = 3 Mm, *Pav* = +5 dBm)

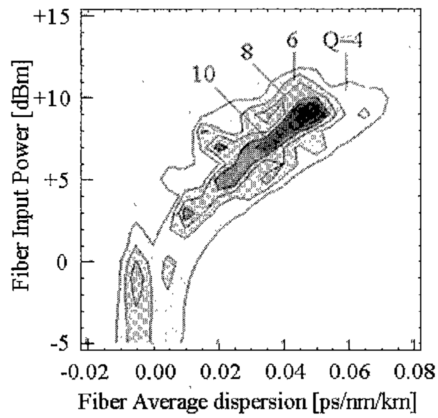

Fig. 9. Q-map on the *Dav-Pav* plane for 40 Gbit/s lines. (Nc = 2, La = 80 km, Lt = 3 Mm, Dc = +30 ps/nm)

The other important point is the location of the dispersion compensation elements. In the dispersion compensated soliton systems, the pulse width becomes minimal around the center point between the dispersion compensation elements, where the frequency chirp becomes zero. If we put the pulse source and the receiver at the chirp-free points, pre-chirping or chirp compensation techniques are not required to get the optimal transmission. Therefore, the location of the dispersion compensation element is important [9].

Fig. 10 shows the calculated pulse widths for 40 Gbit/s transmission lines. The pulse width becomes minimal around the center point of the dispersion compensation spans, where the frequency chirp becomes zero. We can estimate Ts from this figure, about 6 ps for normal dispersion type and about 5 ps for anomalous dispersion type. If we input Dc = ±20ps/nm, S = 1.65 to the equation (4), then we get Ts = 5.6 ps.

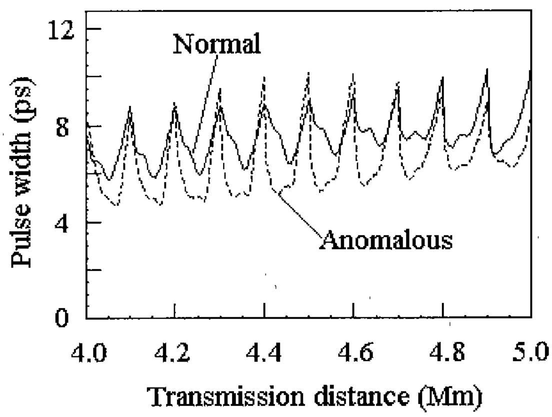

Fig. 10. Pulse width calculation for 40 Gbit/s lines. (Normal: Dc = +20 ps/nm, Anomalous: Dc = -20 ps/nm, Lc = 100 km, Pav = +5 dBm, Dav = +0.03 ps/nm/km)

4. 40 Gbit/s based transmission experiment

4.1 40 Gbit/s, 640 km transmission experiment

We performed 40 Gbit/s, 640 km single-channel dispersion managed soliton transmission experiment using conventional dispersion shifted fibers [10]. Fig. 11 shows the experimental setup. The optical pulse is generated by a mode-locked laser diode (MLLD), and the pulse width is 5.7 ps. This MLLD can be tuned between 1530 nm and 1560 nm wavelength range. The MLLD is triggered by 10 GHz clock signal. The output pulse is modulated by a lithium niobate modulator (LN-mod), and the output 10 Gbit/s, 2^{15}-1 PRBS data pattern is optically multiplexed to 40 Gbit/s signal by a PLC-multiplexer.

The amplifier spacing is 80 km, and each span consists of 4-pieces of 20 km length DSF. The zero-dispersion wavelength of the each fiber is distributed between 1535 nm and 1560 nm. Their standard deviation is 6.1nm. The 2-pieces of dispersion compensation fibers (DCF) of −30 ps/nm and −40 ps/nm are installed in the transmission line. The average zero-dispersion wavelength is 1547.9 nm (without DCF), and 1549.5 nm (with DCF).

The amplifier noise figure is 5 dB, and no-filter is used in each amplifier. The fiber loss rate is 0.21 dB/km, and the dispersion slope is 0.07 ps/nm^2/km. The average dispersion of the transmission line can be changed according to the laser-wavelength. In the receiver, 10 GHz clock signal is recovered by the 40 GHz phase locked loop circuit (PLL), and the 40 Gbit/s data stream is demultiplexed to a 10 Gbit/s signal using an electroabsorption modulator (EA-mod).

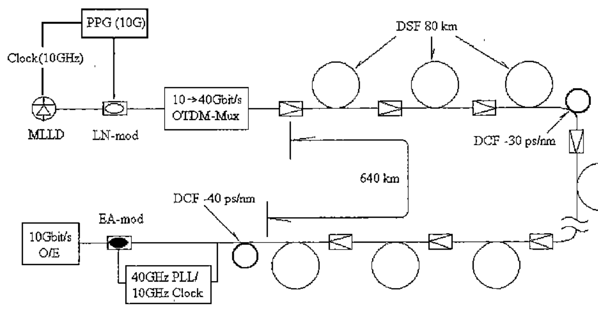

Fig. 11. Experimental setup of the 40 Gbit/s, 640 km line.

Fig.12 shows the observed pulse widths by a streak camera in two different types of dispersion compensation lines. In case (a), the DCFs are installed in the end of the compensation spans, 320 km and 640 km (end DCF allocation). In case (b), these are installed in the center of the spans, 160 km and 480 km (center DCF allocation). The signal power is +7 dBm, which is the optimal power in these cases. The average pulse widths at the receiver for 1549.2 nm to 1550.4 nm signals are 20.2 ps in case (a) and 8.8 ps in case (b). The pulse broadening is suppressed and intersymbol interference (ISI) is reduced in case (b).

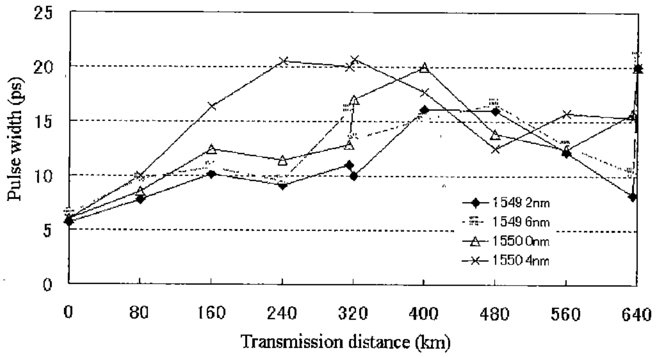

(a) End DCF allocation: 320 km, 640 km

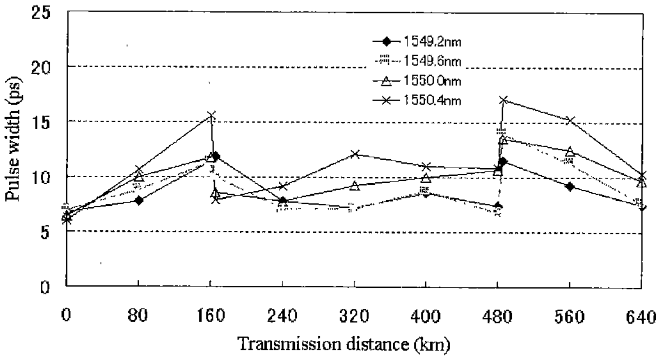

(b) Center DCF allocation: 160 km, 480 km

Fig. 12. Measured pulse width for the two types of dispersion compensation line.

Fig. 13 shows the power dependence of the wavelength tolerance for the end DCF allocated line. The optimal power is +7 dBm and wavelength tolerance is 0.4 nm.

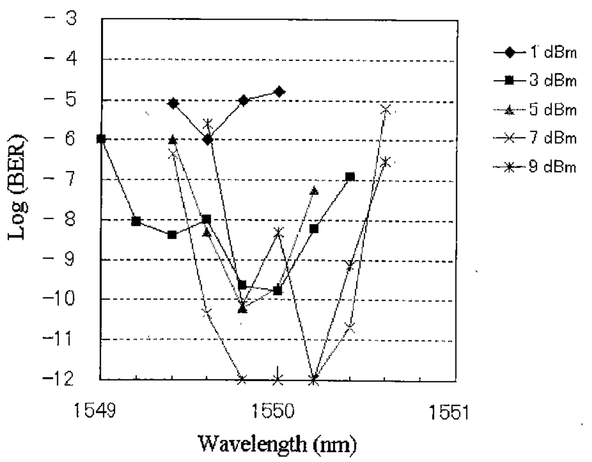

Fig. 13. Wavelength tolerance for each signal power in the end DCF allocated line.

Fig. 14 shows the measured bit error rate for the two types of lines with optimal power of +7 dBm. In the case (b), the error-free transmission is observed in the wavelength range of 1.2 nm: 1549.4 nm - 1550.6 nm, expanded 3 times compared to the case (a). The calculated average dispersion tolerance is 0.084 ps/nm/km which means the accumulated dispersion tolerance is 54 ps/nm.

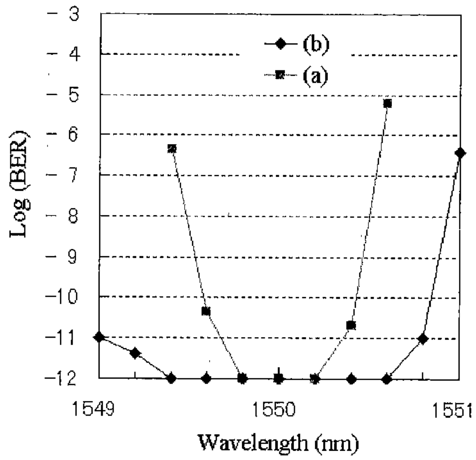

Fig. 14. Transmission improvement by the DCF allocation.

Fig.15 shows the calculated Q-maps for the two types of lines. The amplifier noise figure is +5 dB. The optimal signal power is about +7 dBm and agrees well with the experimental result. The dispersion tolerances for error-free transmissions (BER < 10^{-12}, Q > 7) are 0.03 ps/nm/km for case (a), and 0.09 ps/nm/km for case (b). This values are correlate well with the experimentally observed wavelength tolerance of 0.4 nm and 1.2 nm, that mean the dispersion tolerances of 0.028 ps/nm/km and 0.084 ps/nm/km, respectively.

Fig. 16 shows the Q-maps on initial chirp parameter C – Dc plane. The average dispersion is fixed to +0.03 ps/nm/km. The DCFs are installed at the end point of the compensation spans in the case (a), and they are installed at the center point of the compensation spans in case (b). In case (b), we get larger Dc tolerance and better transmission quality has achieved without initial frequency chirp. In the case (a), $C > 0$ (down-chirping) is required for the normal dispersion type, and $C < 0$ (up-chirping) is required for the anomalous dispersion type.

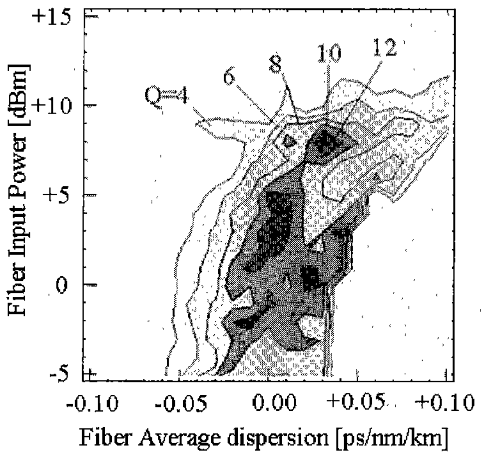

(a) End DCF allocation: 320 km, 640 km

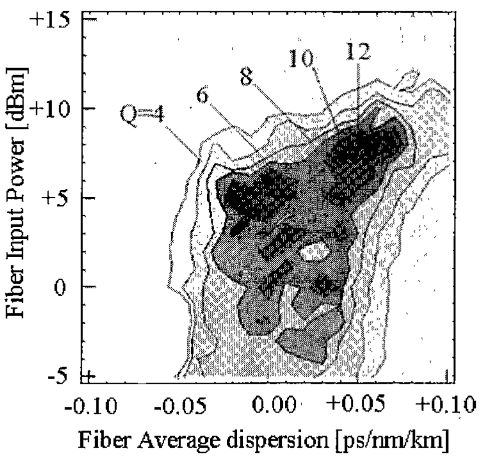

(b) Center DCF allocation: 160 km, 480 km

Fig. 15. Q-map for the 40 Gbit/s, 640 km line. ($Nc = 4$, $Dc = -35$ ps/nm, $La = 80$ km, $NF = 5$ dB)

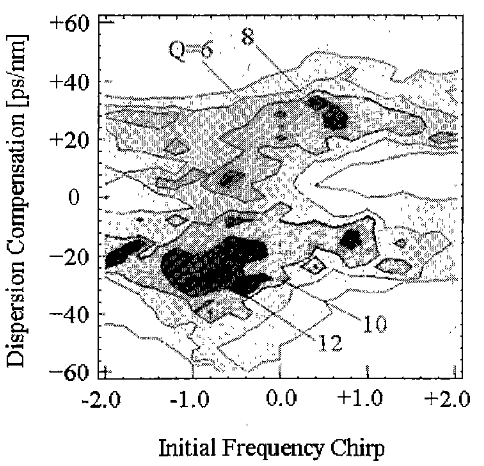

(a) End DCF allocation: 320 km, 640 km

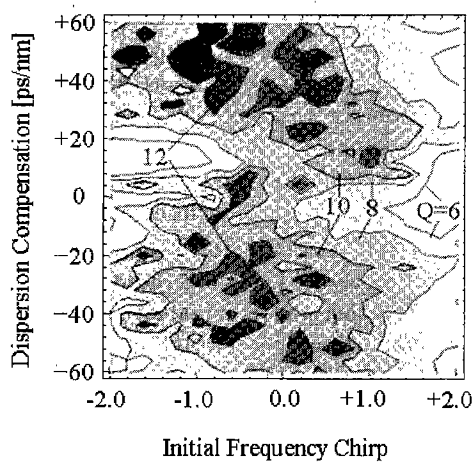

(b) Center DCF allocation: 160 km, 480 km

Fig. 16. Q-map for the 40Gbit/s, 640km transmission line. ($Nc = 4$, $Dav = +0.03$ ps/nm/km, $La = 80$ km, $NF = 5$ dB)

4.2 80 Gbit/s, 800 km transmission experiment

It is difficult to transmit 80 Gbit/s single-channel nonlinear pulses in the conventional DSF [11] [12]. One reason is the dispersion slope. In the soliton-based systems, the amplifier spacing La should be longer than the dispersion length L_d and L_d' [13].

$$L_d = 0.251 \frac{T^2}{D} \qquad L_d' = 0.112 \frac{T^3}{sl} \tag{5}$$

, where L_d(km) and L_d'(km) are the dispersion lengths of 2nd and 3rd order dispersion terms, T(ps) is the pulse width (FWHM), D (ps/nm/km) is the fiber dispersion and sl (ps/nm^2/km) is the dispersion slope. Fig. 17 shows the calculated dispersion length for each pulse width. In 80 Gbit/s single-polarization systems, the pulse width T is about 3 ps, and L_d' becomes critical for conventional fibers of $sl = +0.07$ ps/nm^2/km, and slope compensation is required.

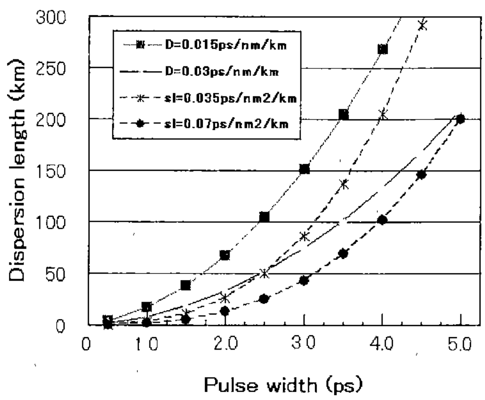

Fig. 17. Dispersion lengths L_d and L_d'.

In over 100 Gbit/s TDM systems, we should employ dispersion slope compensation technique and dense dispersion management technique to maintain the optimal S-parameter value [14] [15]. We can transmit 80 Gbit/s single-channel signals with ordinary DSF by combining the polarization division multiplexing (PDM) technique and 40 Gbit/s TDM technique [16].

Fig. 18 shows the experimental setup. The 40 Gbit/s linearly polarized signal is divided into two channels by a 3 dB optical coupler and adjustable time delay unit is inserted in one channel. Then, they are multiplexed by a polarization beam splitter (PBS) with orthogonal polarization condition. By adjusting the optical delay unit, two signals are interleaved.

The 800 km transmission line consists of 12 DSF spans and one NZ-DSF span. The span length of the DSF is 60 km. Optical filters with a 3 nm bandwidth are included in the EDFA 5, 10 and 14 to suppress ASE originating from the EDFA's. DCF's of -30 ps/nm are inserted after the DSF at every odd span. The average dispersion of each span is set to be roughly the same in order to make the dispersion management easy.

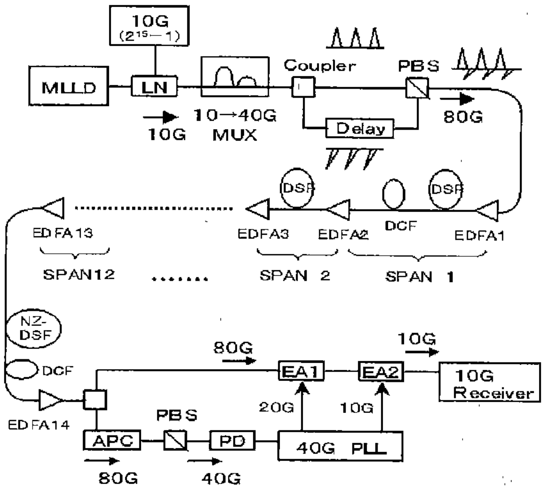

Fig. 18. Experimental setup of the 80Gbit/s, 800km line.

At the receiver, clock is recovered as follows. Branched 80 Gbit/s pulse train is incident on the PBS after adjustment of the polarization state by an automatic polarization controller (APC). Thus, the 80 Gbit/s signal is demultiplexed into the 40 Gbit/s signal according to the polarization discrimination. Locking a 40 GHz phase locked loop (PLL) to an output of the pin-PD, the clock is obtained. Another 80 Gbit/s optical signal is demultiplexed to 10 Gbit/s signals using two EA modulators. The EA modulators are driven at frequencies of 20 GHz and 10 GHz, respectively, synchronized with the 40 GHz PLL. Bit error rates (BER) are measured for these 10 Gbit/s signals. Fig. 19 shows the BER after 800 km transmission, and observed error-free in all channels. The optimal signal power was +7.5 dBm.

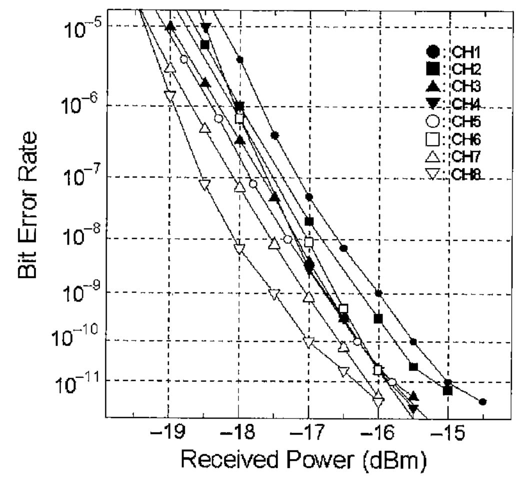

Fig. 19. BER of the 800km transmission.

The dispersion tolerance at distances of 480 km, 600 km and 720 km are evaluated by measuring the BER for the same received power. It is found that the dispersion tolerance is about 15ps/nm, and this value is about 1/3 of the single polarization 40 Gbit/s case. This is because the polarization-mode dispersion (PMD) causes timing jitter and degrades the orthogonal signals.

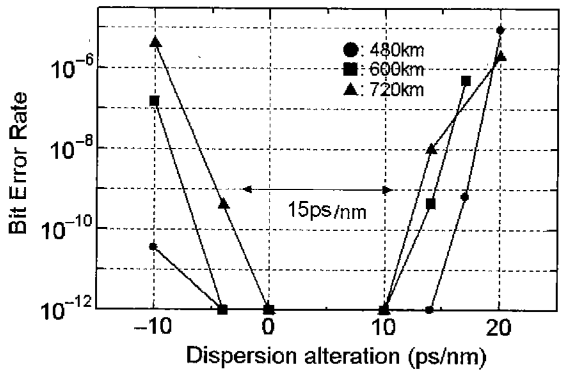

Fig. 20. Dispersion tolerance for each section.

5. Conclusion

We show the effectiveness of Q-maps for the design of high-speed TDM systems. In the 40 Gbit/s systems, we confirmed the optimal dispersion compensation ***Dc*** is always about ±30 ps/nm in 40 Gbit/s systems. We observed error-free transmission in the wavelength range of 1.2 nm in 640 km transmission experiment, by optimizing the location of the dispersion compensation fibers. The transmissible condition shows good agreement with the numerical results. We performed 80 Gbit/s (40 Gbit/s, 2 PDM), 800 km transmission experiment using conventional DSF and observed error-free transmission. The dispersion tolerance is about 1/3 of the single-polarization case, because the PMD degrades the signal.

We think these single-channel soliton-based systems have advantages in real systems, because (1) soliton stability and higher signal power enables stable long-distance transmission, (2) conventional DSF without any dispersion slope compensation can be used, (3) narrow-band low-cost amplifiers with band pass filters can be used, and (4) design of the dispersion map of the line is simple and not so difficult.

6. Acknowledgment

The authors would like to thank Prof. M. Matsumoto of Osaka University for valuable discussions.

(Manuscript received January 26, 2001, revised July 23, 2001)

References

(1) F. Matera and M. Settembre, "Role of Q-factor and time jitter in the performance evaluation of optically amplified transmission systems", IEEE J. Selected Topics in Quantum Electronics, **6**, pp. 308-316, (2000).

(2) E. A. Golovchenko et al., "Modeling of transoceanic fiber-optic WDM communication systems", IEEE J. Selected Topics in Quantum Electronics, **6**, pp. 337-347, (2000).

(3) A. Sahara et al., "Q-factor contour mapping for evaluation of optical transmission systems: soliton against NRZ against RZ pulse at zero group velocity dispersion", Electron. Lett. **32**, pp. 915-916, (1996).

(4) I. Morita et al., "40 Gbit/s single-channel soliton transmission over 10200 km without active inline transmission control", ECOC'98, Madrid, Spain, (1998).

(5) N. S. Bergano et al., "Margin measurements in optical amplifier systems", IEEE Photon. Technol. Lett., **5**, pp. 304-306, (1993).

(6) K. Shimoura and S. Seikai, "Two extremely stable conditions of optical soliton transmission in periodic dispersion compensation lines", IEEE Photon. Technol. Lett., **11**, pp. 200-202, (1999).

(7) T. Yu et al., "Dispersion-managed soliton interactions in optical fibers", Opt. Lett., **22**, pp. 793-795, (1997).

(8) G. P. Agrawal, "Nonlinear fiber optics", chap. 5, Academic Press, (1989).

(9) N. J. Smith et al., Electron. Lett., **32**, pp. 54-55, (1997).

(10) K. Shimoura et al., "Location effect of dispersion compensation elements in 40 Gbit/s soliton transmission line", ECOC2000, Munich, **9.1.5**, (2000.9).

(11) M. Nakazawa et al., "80 Gbit/s soliton data transmission over 500 km with unequal amplitude solitons for timing clock extraction", Electron. Lett., **30**, pp. 1777-1778, (1994).

(12) S. Kawanishi et. al., "100 Gbit/s, 560 km optical transmission experiment with 80 km amplifier spacing employing dispersion management", Electron. Lett., **32**, pp470-471, (1996).

(13) A. Hasegawa and Y. Kodama, "Solitons in Optical Communications", chap. 7, Oxford University Press, (1995).

(14) A. H. Liang et al., "High-speed soliton transmission in dense periodical fibers", Opt. Lett. **24**, 799-801, (1999).

(15) H. Anis et al., "Continuous dispersion managed fiber for very high speed soliton systems", ECOC'99, Nice, France, (1999).

(16) I. Yamashita et al., "Single channel 80 Gbit/s OTDM transmission through a 800 km dispersion shifted fiber", ECOC2000, Munich, **6.1.5**, (2000.9).

Kazuhiro Shimoura (Member) received B.E. and M.E. degrees in electrical engineering from Osaka University in 1986 and 1988, respectively. In 1988, he joined the Kansai Electric Power Co., Inc. and now a senior researcher. His interests are numerical modeling of optical communication lines and information system design as the social interface for researchers. He is a member of IEE and IEICE.

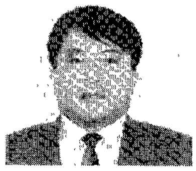

Ikuo Yamashita (Member) received B.E. and M.E. degrees in communication engineering from Osaka University in 1988 and 1990, and Ph.D. degrees from Osaka Prefecture University in 2000. In 1990, he joined the Kansai Electric Power Co., Inc. and now a senior researcher. His interests are optical amplification and nonlinear phenomena in fibers. He is a member of IEE and IEICE.

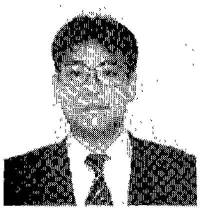

Shigeyuki Seikai (Member) received B.E., M.E. and Ph.D. degrees in communication engineering from Osaka University in 1969, 1971 and 1974, respectively. In 1974, he joined the NTT Corporation and form 1987 to 1990 he was a Professor of Ritsumeikan University. In 1991, he joined the Kansai Electric Power Co., Inc. and now a chief researcher. His interests are nonlinear optics and optelectronics. He is a member of IEE, IEICE and OSA.